

# SHORT-RANGE REPULSION IN THE SINGLET ELECTRONIC EXCITED STATES OF Zn-RG AND Cd-RG COMPLEXES: HOW MUCH OF VAN DER WAALS INTERACTION?



Jagiellonian University

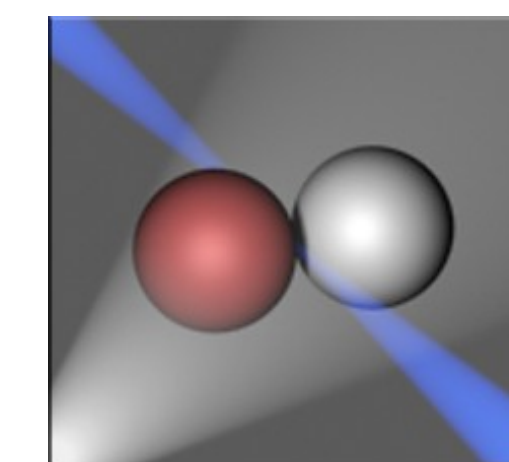
The 20<sup>th</sup> International Conference on High Resolution Molecular Spectroscopy  
Prague, Czech Republic  
September 2-6, 2008

M. STROJECKI<sup>a,†</sup>, M. KROŚNICKI<sup>b</sup>, J. KOPERSKI<sup>a</sup>

<sup>a</sup> Smoluchowski Institute of Physics, Jagiellonian University, Reymonta 4, 30-059 Kraków, Poland

<sup>b</sup> Institute of Theoretical Physics and Astrophysics, University of Gdańsk, Wita Stwosza 57, 80-952 Gdańsk, Poland

<sup>†</sup>e-mail: strojecki@o2.pl



Molecular Laser Spectroscopy Group  
Institute of Physics



University of Gdańsk

## ABSTRACT

The supersonic beam technique combined with methods of laser spectroscopy have been applied to determine the repulsive wall of the  $D^1\Sigma^+$  ( $\Omega=0$ ) excited-state potential of Zn-RG (RG=Ne, Ar, Kr) [1] and Cd-RG complexes (RG=He [2], Ne [2], Ar [3], Kr [3], Xe [2]). The complexes were produced in a continuous free-jet expansion beam and excited with a dye-laser beam directly from the  $X^1\Sigma^+$  ( $\Omega=0$ ) to the excited state (see Fig. 2). A total laser induced fluorescence (LIF) signal was recorded with a photomultiplier (for details of the experimental procedure see [3] and Fig. 1).

Analysis of the LIF signal in the form of the unstructured continuum-bound profiles, recorded for the first time in the excitation using the  $D^1\Sigma^+ \leftarrow X^1\Sigma^+$  transition, yielded information on the short-range  $D^1\Sigma^+$ -state potential of the complexes. A comparison between the  $D^1\Sigma^+$ -state repulsive branches of the ZnNe and CdNe, ZnAr and CdAr, and ZnKr and CdKr, as well as comparison with the results of *ab initio* calculations [4,5] yielded information on a character of the bonding in this region of internuclear separations (*i.e.*,  $R=3.5-5$  Å). Besides of the increasing repulsion that increases with RG-atom ground-state  $\alpha_{RG}$  polarizability ( $\alpha_{He} < \alpha_{Ne} < \alpha_{Ar} < \alpha_{Kr} < \alpha_{Xe}$ ) [6] we also found that the repulsion depends on the atomic excited-state  $\alpha_{Zn}$  and  $\alpha_{Cd}$  polarizabilities of the asymmetrical electron density distribution of metal atom. This indicates a similar behaviour as in the ground states of the Zn-RG and Cd-RG molecules [7], that are dominated by van der Waals interaction with an admixed covalent contribution in the short-range region (see Table 1).

## BIBLIOGRAPHY:

- [1] M. Strojecki, M. Krośnicki and J. Koperski, „Short-range repulsion in the  $D^1\Sigma^+$ -state potential of the ZnRg (Rg = Ne, Ar, Kr) complexes determined from a direct free-bound excitation at the  $D^1\Sigma^+ \leftarrow X^1\Sigma^+$  transition”, to be published  
[2] M. Strojecki, M. Krośnicki, M. Łukomski and J. Koperski, „Excitation spectra of Cd-rare gas complexes recorded at the  $D^1\Sigma^+ \leftarrow X^1\Sigma^+$  transition: from the heaviest CdXe to the lightest CdHe”, to be published  
[3] M. Ruzscaak, M. Strojecki, and J. Koperski, *Chem. Phys. Lett.*, **416**, 147-151 (2005)  
[4] E. Czuchaj, M. Krośnicki and H. Stoll, *Theor. Chem. Acc.*, **105**, 219-226 (2001)

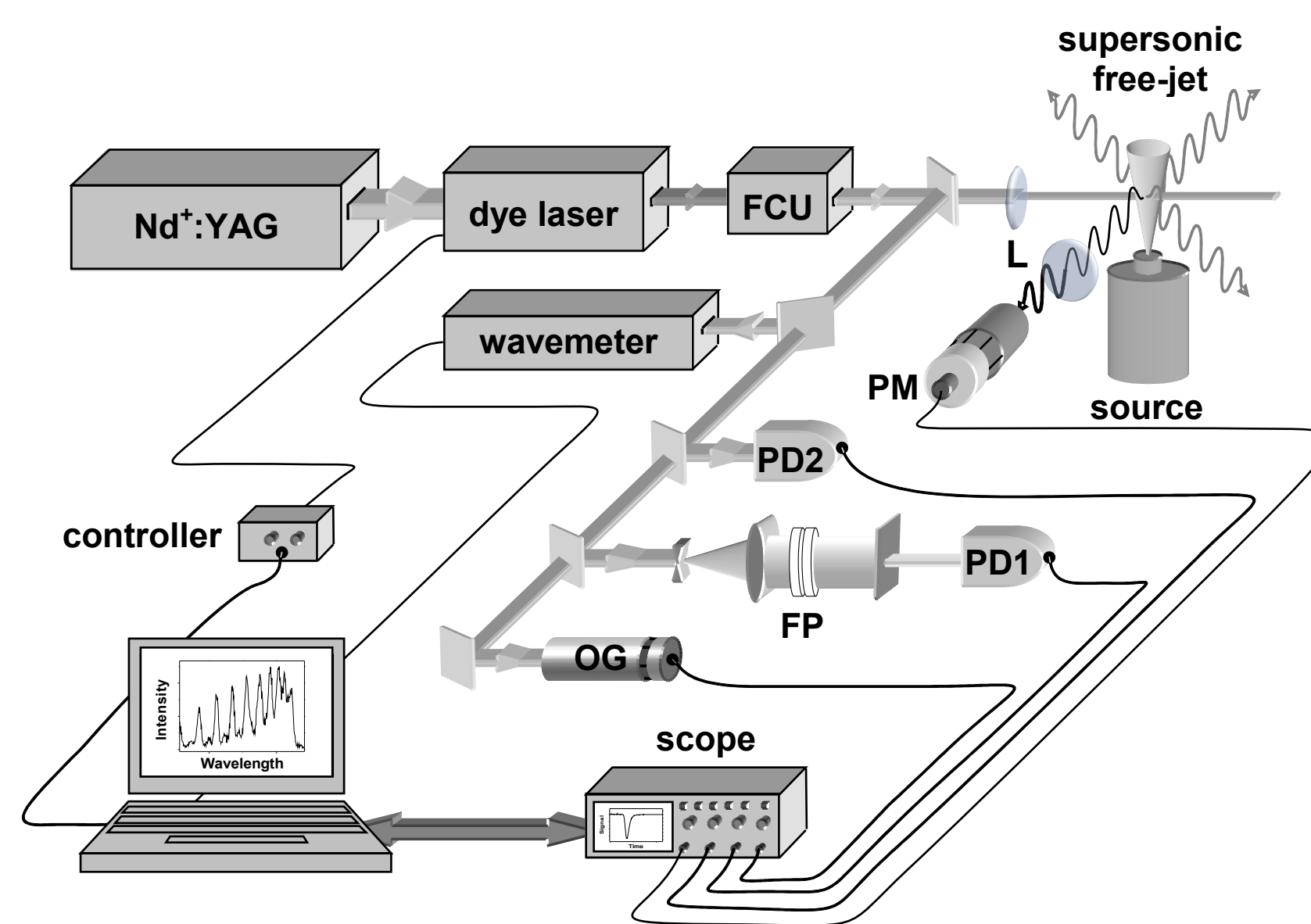


Fig. 1. Scheme of the experimental set-up FCU – Frequency Conversion Unit, L – lenses, OG – Argon filled optogalvanic cell, PD1, PD2 – photodiodes, FP – Fabry-Perot etalon, PM – photomultiplier tube. Perpendicular directions between laser beam, molecular supersonic expansion beam and direction of observation allow reducing a Doppler broadening.

- [5] E. Czuchaj, M. Krośnicki, H. Stoll, *Chem. Phys.*, **265**, 291-299 (2001)  
[6] T. M. Miller and B. Bederson, *Adv. At. Mol. Phys.*, **13**, 1-55 (1977)  
[7] J. Koperski, „Van der Waals Complexes in Supersonic Beams. Laser Spectroscopy of Neutral-Neutral Interactions”, Wiley-VCH, Weinheim, (2003)  
[8] D. J. Funk, A. Kvaran, W. H. Breckenridge, *J. Chem. Phys.*, **90** (1989) 2915  
[9] I. Wallace, J. G. Kaup, W. H. Breckenridge, *J. Phys. Chem.*, **95** (1991) 8060  
[10] J. G. Kaup, W. H. Breckenridge, *J. Phys. Chem.*, **99** (1995) 13701

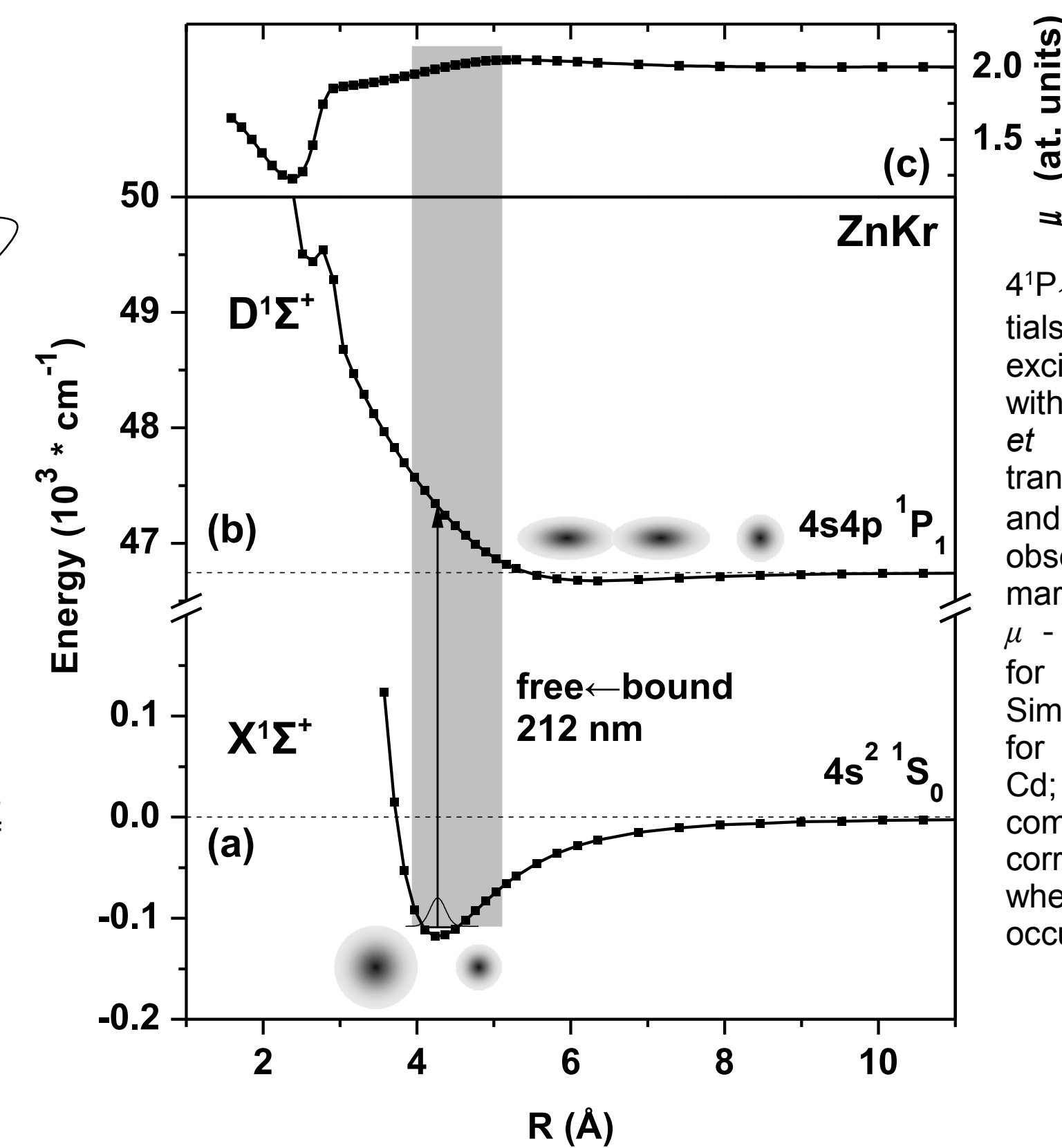


Fig. 2. Potential energy curves (PEC) and their associated orbital interactions drawn for the (a)  $X^1\Sigma^+$  ground as well as (b)  $D^1\Sigma^+$  excited state of ZnKr correlated with the  $4^1P_1$  atomic asymptote. Potentials of the ground  $X^1\Sigma^+$  and excited states are represented with *ab initio* points of Czuchaj *et al.* [5]. The free-bound transition between the ground and  $D^1\Sigma^+$  excited state observed in the experiment are marked with vertical arrows; (c)  $\mu$  - transition dipole moments for the  $D^1\Sigma^+ \leftarrow X^1\Sigma^+$  transition. Similar schemes can be drawn for the other MeRG (Me=Zn, Cd; RG=He, Ne, Ar, Kr, Xe) complexes. Grey area corresponds to the region where free-bound transitions occur.

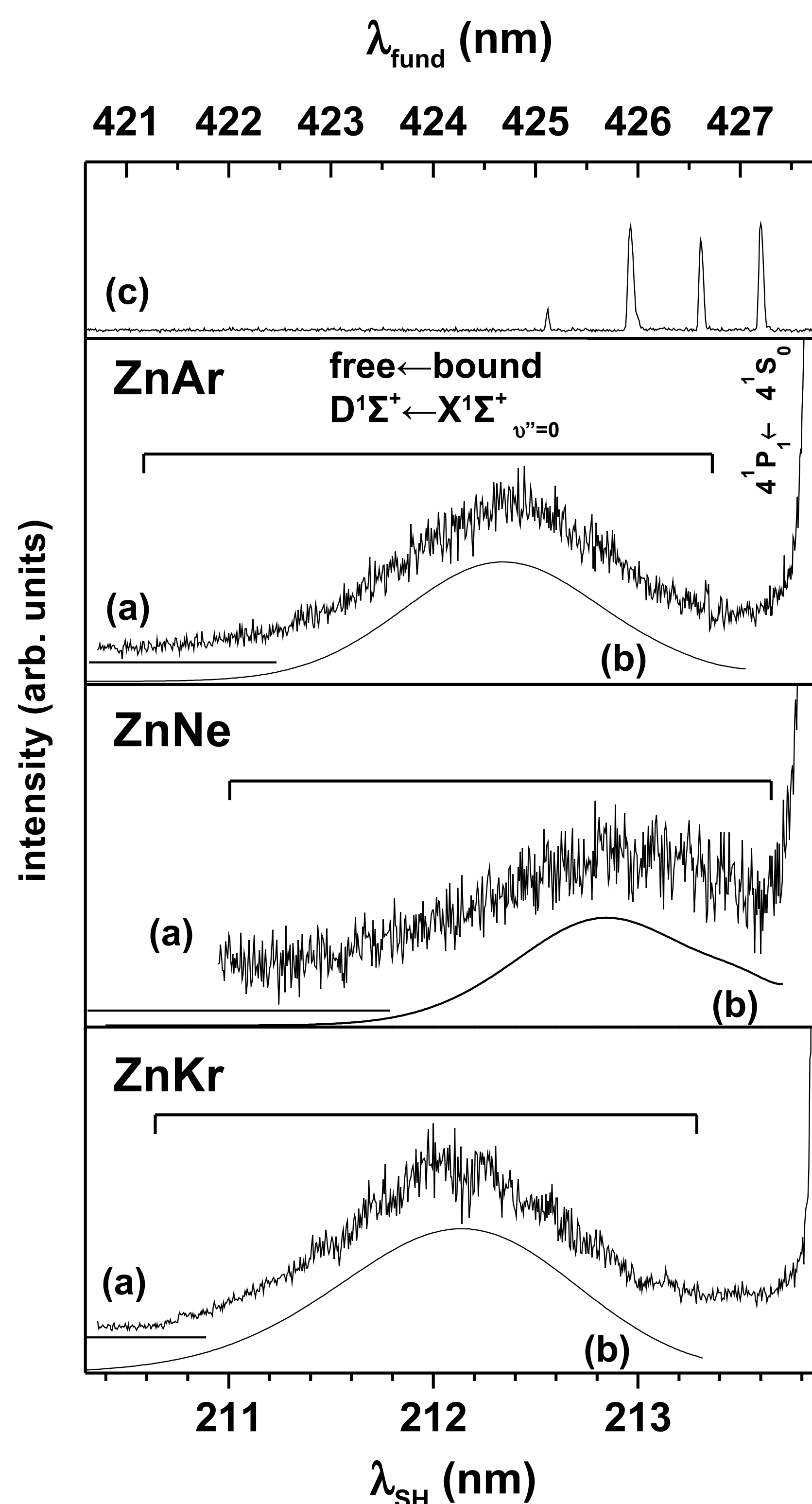


Fig. 3. The LIF excitation spectra of ZnAr, ZnNe and ZnKr recorded in the experiment. (a) Total LIF spectrum to the blue from the  $4^1P_1 \leftarrow 4^1S_0$  Zn atomic transition corresponding to the  $D^1\Sigma^+ \leftarrow X^1\Sigma^+$  ( $v''=0$ ) free-bound transitions. (b) Simulation of the unstructured profile in which Morse representations for the  $X^1\Sigma^+$  [7] and  $D^1\Sigma^+$  states were used (see Table 1),  $\mu(R)=1$  was used during the simulation. (c) Optogalvanic signal from an Ar-filled hollow cathode lamp recorded as a function of wavelength corresponding to the fundamental laser frequency; the identified ArI lines are: 425.120, 425.936, 426.629, 427.217 nm.

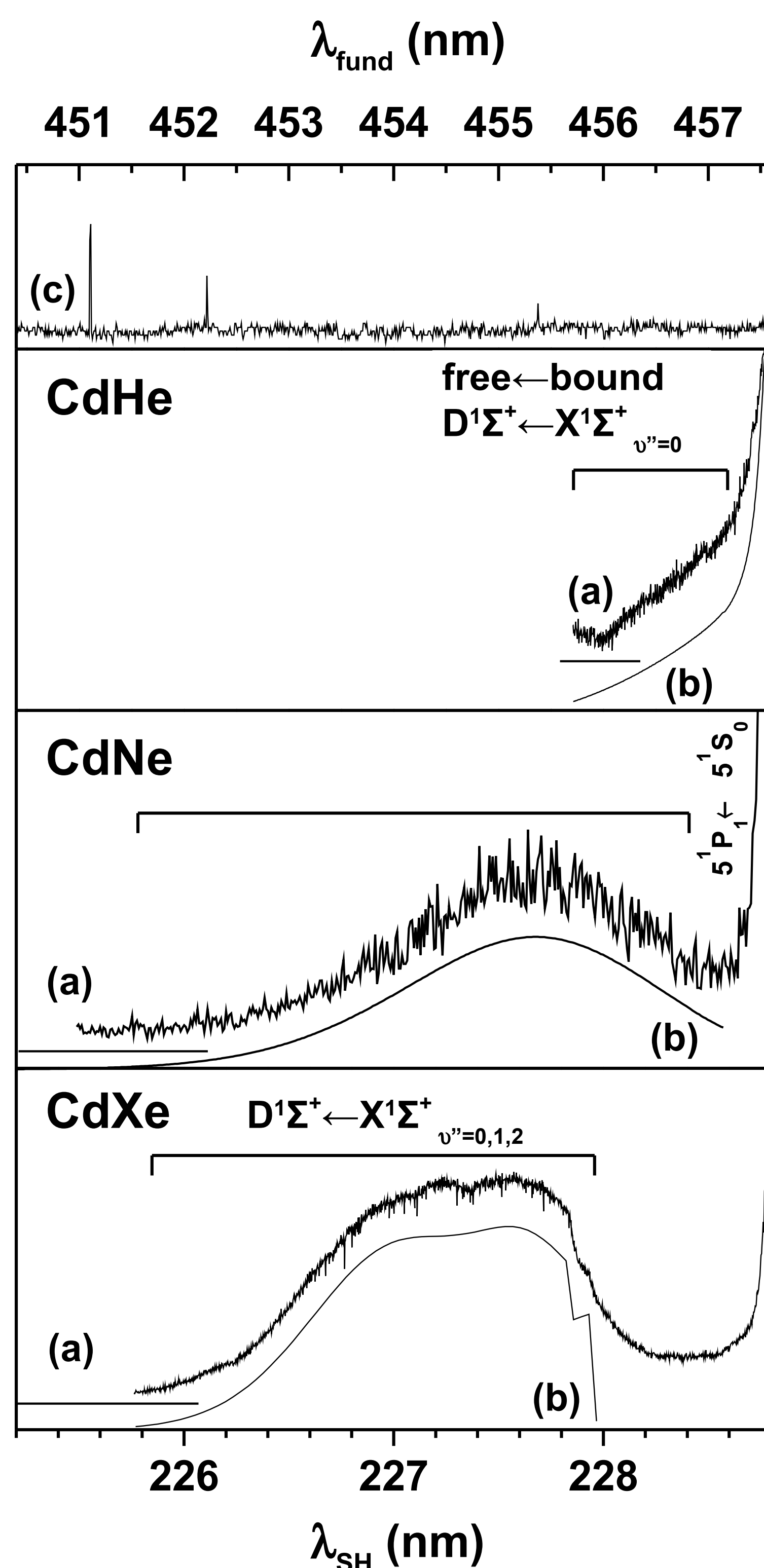


Fig. 4. The LIF excitation spectrum of CdHe, CdNe and CdXe recorded in the experiment. (a) Total LIF spectrum to the blue from the  $5^1P_1 \leftarrow 5^1S_0$  Cd atomic transition corresponding to the  $D^1\Sigma^+ \leftarrow X^1\Sigma^+$  ( $v''=0$ ) free-bound transitions. (b) Simulation of the unstructured profile corresponding to the  $D^1\Sigma^+ \leftarrow X^1\Sigma^+$  free-bound transition in which Morse representations for the  $X^1\Sigma^+$  [7] and  $D^1\Sigma^+$  states were used (see Table 1). For CdXe transitions from ( $v''=0, 1, 2$ ) are also included.  $\mu(R)=1$  was used during the simulation. (c) Optogalvanic signal from an Ar-filled hollow cathode lamp recorded as a function of wavelength corresponding to the fundamental laser frequency; the identified ArI lines are: 451.073, 452.232, 455.432 nm.

	ZnHe <sup>a</sup>	CdHe <sup>a</sup>	ZnNe <sup>a</sup>	CdNe <sup>a</sup>	ZnAr <sup>a</sup>	CdAr <sup>a</sup>	ZnKr <sup>a</sup>	CdKr <sup>a</sup>	ZnXe <sup>a</sup>	CdXe <sup>a</sup>
$D_e$ (cm <sup>-1</sup> )	2.1	8.2	19	38	48	70.5 <sup>b</sup>	64	103.3 <sup>b</sup>	134 <sup>c</sup>	155
$R_e$ (Å)	7.69	8.10	7.60	6.90	6.88	6.48 <sup>b</sup>	6.30	5.66 <sup>b</sup>	5.85 <sup>c</sup>	5.33
$\beta/10^6$ (Å <sup>-1</sup> )	-	0.49	0.50	0.52	0.52	0.54 <sup>b</sup>	0.63	0.72 <sup>b</sup>	0.71 <sup>c</sup>	0.77
$A'$ (cm <sup>-1</sup> )	-	1.9·10 <sup>4</sup>	9.5·10 <sup>4</sup>	1.1·10 <sup>5</sup>	1.6·10 <sup>5</sup>	1.78·10 <sup>5</sup> <sup>b</sup> -4.5979 <sup>d</sup>	5.1·10 <sup>5</sup>	2.66·10 <sup>6</sup> <sup>b</sup> 1.4731·10 <sup>6</sup> <sup>d</sup>	1.0·10 <sup>6</sup> <sup>f</sup>	4.8·10 <sup>7</sup>
$b'$ (Å <sup>-1</sup> )	-	1.05	1.30	1.36	1.38	1.42 <sup>b</sup> -0.6758 <sup>d</sup>	1.65	2.103 <sup>b</sup> 1.5399 <sup>d</sup>	1.725 <sup>f</sup>	2.76
$C_0$ (Å <sup>-1</sup> )	-	12	40	40	80	110 <sup>b</sup>	80	132 <sup>b</sup>	-	90
$\Delta R=R_e' - R_e''$ (Å)	3.23	3.50	3.18	2.58	2.50	2.17	1.94	1.39	1.47	1.08

<sup>a</sup> this work; <sup>b</sup> Ref. [3]; <sup>c</sup> Ref. [5]; <sup>d</sup> Ref. [8]; <sup>e</sup> Ref. [9]; <sup>f</sup> Ref. [10]

Table 1. Parameters of Morse  $D_e(1-e^{-\beta(R-R_e)})^2$  and shifted Born-Mayer  $A'e^{-\beta R}C_0$  functions used as representations of the  $D^1\Sigma^+$ -state potential energy curve of MeRG complexes. Parameters listed for ZnNe, ZnAr, ZnKr and CdHe, CdNe, CdXe complexes were obtained in this work while those for CdAr and CdKr result of our earlier study [3] and that of Funk *et al.* [8]. As for ZnHe and ZnXe there are from [5] and [9,10], respectively.

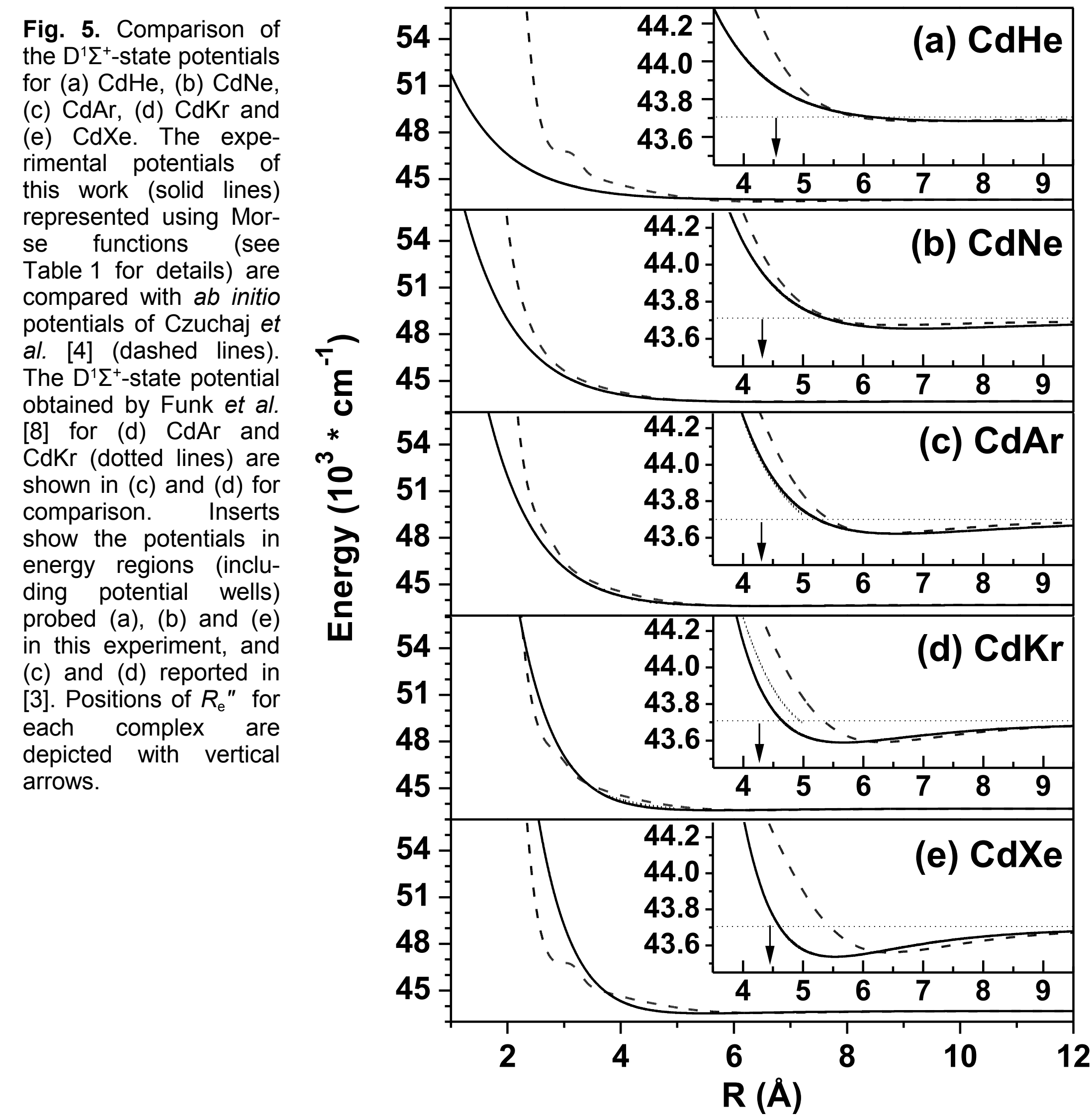


Fig. 5. Comparison of the  $D^1\Sigma^+$ -state potentials for (a) CdHe, (b) CdNe, (c) CdAr, (d) CdKr and (e) CdXe. The experimental potentials of this work (solid lines) represented using Morse functions (see Table 1 for details) are compared with *ab initio* potentials of Czuchaj *et al.* [4] (dashed lines). The  $D^1\Sigma^+$ -state potential obtained by Funk *et al.* [8] for CdAr and CdKr (dotted lines) are shown in (c) and (d) for comparison. Inserts show the potentials in energy regions (including potential wells) probed (a), (b) and (e) in this experiment, and (c) and (d) reported in [3]. Positions of  $R_e''$  for each complex are depicted with vertical arrows.

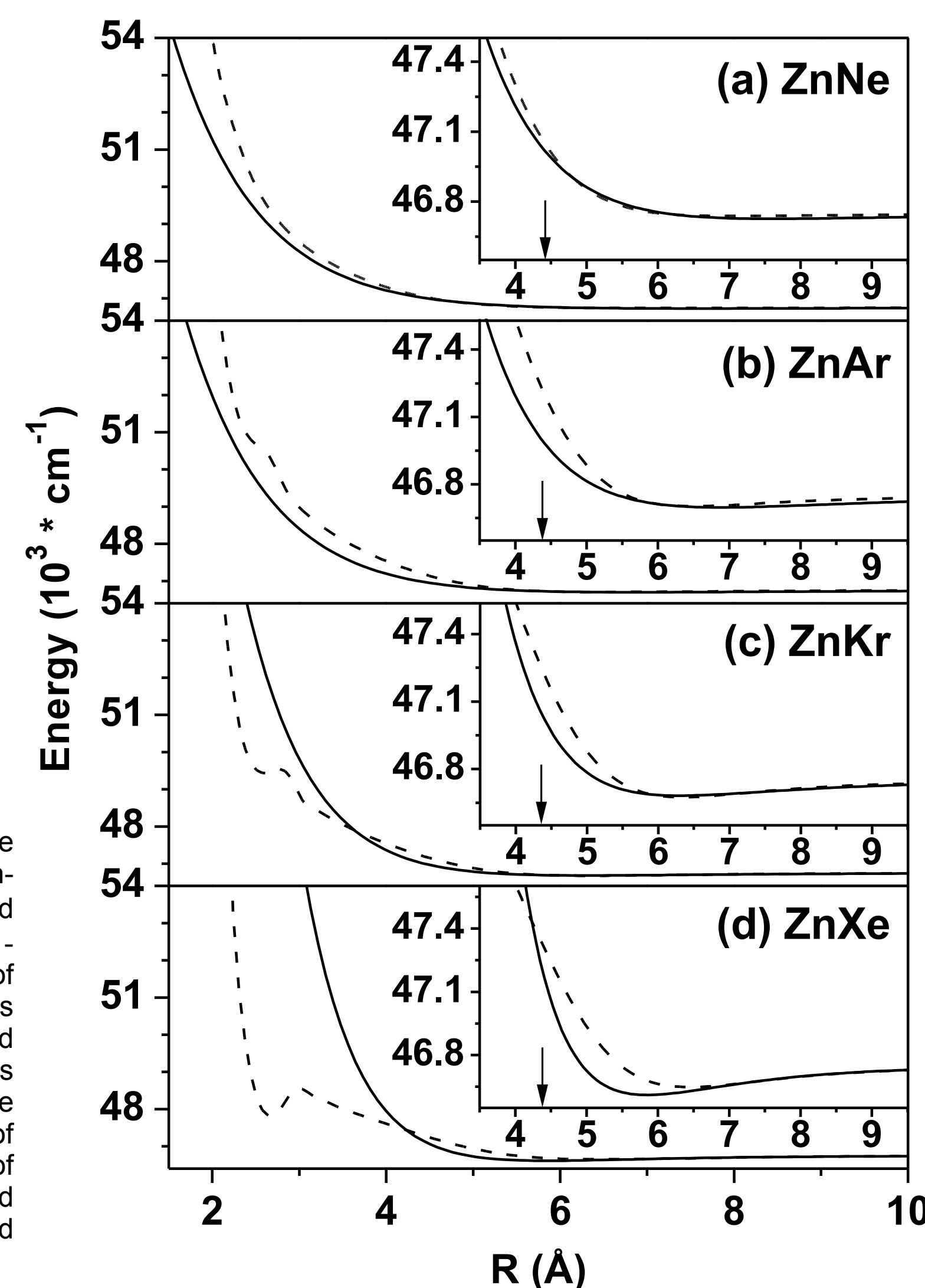


Fig. 6. Comparison of the  $D^1\Sigma^+$ -state potentials obtained for (a) ZnNe, (b) ZnAr and (c) ZnKr. The experimental potentials of this work (solid lines) represented using Morse functions (see Table 1. for details) are compared with *ab initio* potentials of Czuchaj *et al.* [5] (dashed lines). The  $D^1\Sigma^+$ -state potential obtained for (d) ZnXe by Wallace *et al.* [9] (solid line) and Czuchaj *et al.* [5] (dashed line) are also shown for comparison. Inserts show the potentials in energy regions (including potential wells) probed (a)-(c) in this experiment and (d) in [9]. Positions of  $R_e''$  for each complex are depicted with arrows.